Colloids and Surfaces B: Biointerfaces 75 (2010) 175–178

Contents lists available at ScienceDirect

Colloids and Surfaces B: Biointerfaces

journal homepage: www.elsevier.com/locate/colsurfb

Blue orange light emission from biogenic synthesized silver nanoparticles using *Trichoderma viride*

Mohammed Fayaz[a,*], C.S. Tiwary[b], P.T. Kalaichelvan[a], R. Venkatesan[c]

[a] *CAS in Botany, University of Madras, Guindy Campus, Chennai 600 025, India*
[b] *Department of Physics, National Institute of Technology, Durgapur, West Bengal, India*
[c] *National Institute of Ocean Technology, Ministry of Earth Sciences, Chennai, India*

ARTICLE INFO

Article history:
Received 7 November 2008
Received in revised form 28 July 2009
Accepted 17 August 2009
Available online 25 August 2009

Keywords:
Biogenic
FTIR
Trichoderma viride
Silver nanoparticles
Photoluminescence

ABSTRACT

Recent advances in nanomaterial have produced a new class of fluorescence labels by conjugating noble metal with biomolecules. The nanometer size metal conjugates are water soluble, biocompatible and provide important advantage over the florescence dyes. In this regard we synthesized silver nanoparticles at the size of 2–4 nm using biological route and studied fluorescence property of these nanoparticles. We observe that these silver (Ag^+) ions when exposed to filtrate of *Trichoderma viride* are reduced in solution, thereby leading to the formation of an extremely stable silver hydrosol. These silver nanoparticles were characterized by means of UV–vis spectrophotometer, FTIR, HrTEM, EDX, XRD and fluorescence spectroscopy. The nanoparticles exhibit maximum absorbance at 405 nm in UV–vis spectrum. The presence of proteins was identified by FTIR. The HrTEM micrograph revealed the formation of monodispersed spherical nanoparticles and the presence of elemental silver was confirmed by EDX analysis and XRD. These monodispersed silver nanoparticles showed emission in the range of 320–520 nm wavelength.

1. Introduction

In recent years the nanoparticles of II–VI group are very much important due to its emission properties. These nanoparticles (CdS, ZnS, CdSe, etc.) are used for wide range of application in the field of cathode ray tube, flat-panel display, sensor, laser devices, etc. [1–5]. But for biological application these particles are not very successfully applicable. On the other hand, the intense light emission properties of noble metals (gold, silver, etc.) nanoparticles have caught a lot of attention. These nanoparticles are extensively used for biological labeling [6], easy to prepare and have a good chemical and thermal stability [7].

Silver (Ag) nanoparticles (noble metal) have potential application in electronics, optoelectronics [8], in heterogeneous catalysis [9], and surfaces of heat exchange, gas sensors and as conductive inks [10]. But a limited amount of attention has been given to the luminescence from Ag nanoparticles due to its very low efficiency. The absence of band gap makes luminescence exceedingly improbable for these nanoparticles [11]. It was reported that Ag nanoparticles emits light in rare gas matrix at cryogenic temperature under photo activation or electro activation and this photoluminescence was attributed to sp to sp like transition analogy to inter-band transition in bulk silver [12]. The optical properties got enhanced due to lanthanide addition [13]. But for biological application apart from luminescence synthesis method is also equally important. There are many methods for synthesis of Ag nanoparticles are reported, including both chemical and biological methods. In recent times, scientist has endeavored microorganisms as possible eco-friendly nano-factories, for synthesis of silver nanoparticles. The bacterium *Pseudomonas stutzeri* AG259, isolated from silver mine, when placed in a concentrated aqueous solution of $AgNO_3$, played a major role in the reduction of the Ag^+ ions and it makes silver nanoparticles of well-defined size and distinct topography within the *periplasmic* space of the bacteria [14].

While intracellular synthesis in principle may accomplish a better control over the size and shape distributions of the nanoparticles, product harvesting, and recovery are more cumbersome and expensive. The extracellular synthesis by comparison is more adaptable to the synthesis of a wider range of nanoparticles systems [15]. However, optical properties of the biologically synthesized silver nanoparticles have been rarely reported.

In our current investigation, non-pathogenic fast growing fungus *Trichoderma viride*, which habited in dead organic materials, was used for extracellular biosynthesis of silver nanoparticles. The biologically synthesized silver nanoparticles were characterized using UV–vis spectrophotometer (Cary 300 Conc UV–vis spectrophotometer) and fluorescence spectroscopy (PerkinElmer). The size and morphology were characterized using HrTEM (high

* Corresponding author. Tel.: +91 09884466583; fax: +91 44 2352494.
E-mail address: nanofayaz@gmail.com (M. Fayaz).

0927-7765/$ – see front matter © 2009 Elsevier B.V. All rights reserved.
doi:10.1016/j.colsurfb.2009.08.028

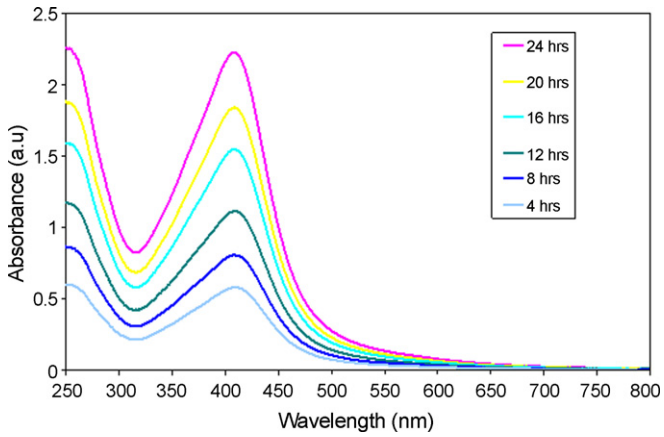

Fig. 1. UV–vis spectrum for silver nanoparticles with different time interval.

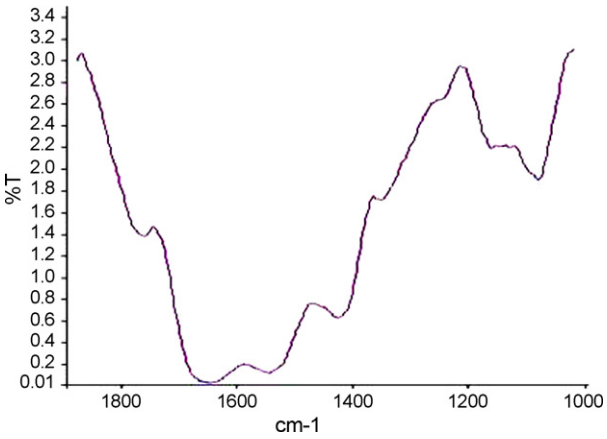

Fig. 2. FTIR spectrum of silver nanoparticles.

resolution transmission electron microscope, Technai 300) with EDS (energy dispersed spectroscopy), XRD (X-ray diffraction, Pan Analytical), and Fourier transformation infrared spectroscopy (PerkinElmer). The PL emission is found to be 320–520 nm with blue color emission along with very narrow range of particle distribution which is stabilized by protein molecules.

2. Experimental details

The fungus *T. viride* was obtained from Culture Collection Center, CAS in Botany, University of Madras, India and maintained in Potato Dextrose Agar slant at 27 °C.

To prepare the biomass for biosynthesis studies the fungi were grown aerobically in liquid broth containing (g/L) KH_2PO_4 – 7; K_2HPO_4 – 2; $MgSO_4{\cdot}7H_2O$ – 0.1; $(NH_2)SO_4$ – 1; yeast extract – 0.6; glucose – 10. The culture flask was incubated in an orbital shaker at 27 °C and agitated at 150 rpm and the biomass was harvested, after 72 h of growth by sieving through plastic sieve followed by extensive washing with sterile double distilled water to remove any medium components from the biomass.

Typically 20 g (wet weight) brought in contact with 100 mL sterile double distilled water for 48 h at 27 °C in an Erlen Meyer flask and agitated as described earlier, after incubation the cell filtrate was obtained by passing it through Whatman filter paper No. 1. In 100 mL cell filtrate, carefully weighed quantity of silver nitrate was added to the Erlen Meyer flask to yield an over all Ag^+ ions concentration of 10^{-3} M in cell filtrate solution and the reaction is carried out in dark condition at 40 °C. The synthesized nanoparticles were dissolved in water and used for measuring optical properties. A thin film is coated on glass plate for measuring the XRD. The water dispersed nanoparticles are seen in HrTEM using carbon coated grid.

3. Results and discussion

The optical properties of silver nanoparticles are related to the excitation of plasma resonance or inter-band transition, particularly on the size effect. The UV–vis absorbance spectrum of colloidal silver can be calculated from the wavelength dependence of optical constant of the particle relative to the surrounding medium using 'MIE' theory. According to 'MIE' theory silver nanoparticles less than diameter 52 nm (electron mean free path of silver) result in a broadening of the plasma absorbance bands, meanwhile the height of the absorbance peak also decreases [16].

Fig. 1 shows the UV–vis spectrum obtained from biologically synthesized silver nano solution. It is observed from the spectra that the silver surface plasmon band occurs at 405 nm in addition to prominent band at around 260 nm. These peaks are characteristic plasmon band for silver nanoparticles [17]. At the initial stage of the reaction, a characteristic absorbance band centered at approximately 405 nm, as reduction proceeds the intensity of the band significantly increased and the full-width at half-maximum (FWHM) of the peak position changed slightly. As there is an increase in the intensity of the absorbance, the concentration of silver particle increases with reaction time. Furthermore there is no significantly different wavelength shift in the absorption spectra at different reaction time interval. The absorbance band at lower wavelength with a good symmetry indicate that the mean diameter of silver nanoparticles is very small with a uniform size distribution. In addition to a prominent band at above 260 nm, it is attributed to electronic excitation in tryptophan and tyrosine residues in protein which indicates the presence of protein molecule in colloidal solution. It is interesting to note from our study that NADPH dependent reductase enzymes, not only specify to *Fusarium oxysporum* as suggested by other [18], but also involves in the reduction of Ag^+ to Ag^0. In case of fungus *T. viride* under experimental condition the possible mechanism suggests that the reduction of Ag^+ to Ag^0 is mainly due to conjugate between the electron shutter with NADPH dependent reductase participation [18].

FTIR spectrum of silver nanoparticles is shown in Fig. 2. This spectrum shows the presence of bands at 1650, 1540, 1423 and 1060 cm^{-1}. The bands at 1650 correspond to primary amine NH band, similarly, 1540 and 1060 corresponds to secondary amine NH band and primary amine CN stretch vibrations of the proteins, respectively [19]. The positions of these bands were close to that reported for native proteins [20]. The FTIR result indicates that the secondary structures of proteins were not affected as a consequence of reaction with Ag^+ ions or binding with silver nanoparticles. The band at 1425 cm^{-1} is assigned to methylene scissoring vibration from the protein in the solution.

XRD pattern taken using Cu Kα target in the range 20–90 of the Ag nanoparticles is shown in Fig. 3. The peaks matches with JCPDF Card No-087-0720. There is no new peak because protein is found in this range. The peak listing is shown in Table 1. The

Table 1
d-Spacing standard and calculated from XRD with the plane.

d_{JCPDF}	$d_{calculated}$	(*h k l*)
2.354	2.321	(1 1 1)
2.0386	2.032	(2 0 0)
1.4415	1.443	(2 2 0)
1.2293	1.231	(3 1 1)
1.177	1.181	(2 2 2)